Binding and Migration Paths of Au Adatoms on the GaAs (001) Surface

Bonapasta, A.A.; Buda, F.

Binding and migration paths of Au adatoms on the GaAs(001) surface

A. Amore Bonapasta*
Consiglio Nazionale delle Ricerche, ICMAT, V. Salaria Km. 29,5-CP 10, 00016 Monterotondo, Scalo, Italy

F. Buda
Department of Theoretical Chemistry, Vrije Universiteit Amsterdam, De Boelelaan 1083, NL-1081 HV Amsterdam, The Netherlands
(Received 21 December 2000; revised manuscript received 26 July 2001; published 2 January 2002)

The binding and the migration paths of an isolated Au adatom on the GaAs (001)-$\beta 2(2\times4)$ reconstructed surface have been investigated by first-principle total-energy calculations in the Car-Parrinello scheme. The potential energy surface calculated for the Au adatom shows that the most interesting Au binding sites are located at short-bridge sites next the As-As dimers of the surface. Similar binding sites were found for Ga adatoms on the same surface. However, the Au chemical binding is *different* from that of Ga. A Ga adatom forms strong covalent Ga-As bonds with a *marked ionic character* when interacting with the As dimers, while the Au-dimer interaction is characterized by the formation of weaker *pure covalent* Au-As bonds. Accordingly, Au adatoms do not break the As-As dimers at variance with the case of Ga adatoms. The characteristics of the Au binding also account for an anisotropic Au migration that results to be faster along the dimer rows than perpendicular to them.

DOI: 10.1103/PhysRevB.65.045308 PACS number(s): 68.35.−p, 68.43.−h, 71.15.Mb

I. INTRODUCTION

The main factors in the degradation of semiconductor devices are the degradation of metal-semiconductor interfaces as well as metal films on the semiconductor surface.[1–3] Generally, metallization schemes involve structures formed by different metals, e.g., Ni/Au/Te, on the semiconductor. The atoms of each metallic species may give rise to degradation processes like exchange with the atoms of the semiconductor as well as lateral diffusion on the semiconductor surface.[2] The quality of the metal contacts is also related to the morphology of the metal films that is fixed by the first steps of the metal deposition. Thus, several technological problems concerning the realization of well-defined metal-semiconductor interfaces or the degradation of metallic contacts are closely related to the interaction of single metal adatoms with a semiconductor surface. Metal adsorption on semiconductor surfaces is also of interest from a fundamental point of view because the deposition of fractions of a metallic monolayer may have significant effects on the surface structure at a microscopic level.[4,5] Gold is used in different metallization schemes. Several experimental studies have shown that Au atoms have a different behavior when interacting with Si or GaAs surfaces. Si-Au alloys are formed at low temperature (80 °C) in the case of the Au/Si(001) system.[6] On the other hand, in the case of Au/GaAs(001), a well-defined Au/GaAs interface is observed at low temperature that becomes rough at 400 °C due to interdiffusion processes.[7] Moreover, Au atoms seem involved in degradation processes of metal-semiconductor contacts that originate from a lateral migration of metallic atoms.[2] All these results have motivated the present study, which is focused on the investigation of the chemical binding and the migration paths of an Au adatom on the GaAs(001)-$\beta 2(2\times4)$ surface. The $\beta 2(2\times4)$ reconstruction model of the GaAs(001) surface has been considered here because it is stable at equilibrium[8,9] and seems to be the dominating surface structure over a wide range of growth conditions.[10,11] This (2×4) surface structure is characterized by two As-As dimers and two missing dimers, see Fig. 1(a). More specifically, on the *top* (first) layer, pairs of As-As dimers form dimer rows in the (110) directions separated by ''channels'' formed by two missing rows of As atoms and by one missing row of Ga atoms on the *second* layer. Rows of As-As dimers are formed in the middle of these channels by the As atoms of the *third* layer of the substrate. Further channels perpendicular to the As-As dimer rows [i.e., in the $(\bar{1}10)$ direction] separate the As-As dimers of the top layer. The chemical binding and the migration paths of an Au adatom on the GaAs(001)-$\beta 2(2\times4)$ surface have been carefully investigated here by performing Car-Parrinello[12,13] (CP) total-energy calculations. More specifically, the adatom-surface interaction has been investi-

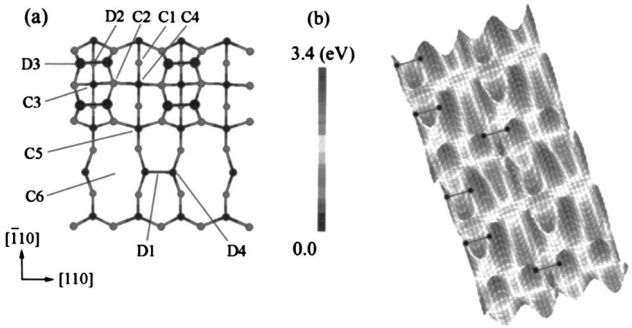

FIG. 1. (a) Stick and ball model of the GaAs (001)-$\beta 2(2\times4)$ surface (top view). The As and Ga atoms are represented by black and gray spheres, respectively. The size of the spheres decreases when going from the top layer to the fourth layer. Different sites for an Au adatom on the surface are shown in the figure: the *D* and *C* letters identify sites close to the As dimers and located in the ''channels'' of the surface, respectively. (b) Perspective view of the potential energy surface (PES) for an Au adatom on the GaAs (001)-$\beta 2(2\times4)$ surface. The figure also shows the positions of some As-As dimers on the surface.

TABLE I. Total energies (electron volts) calculated for an Au adatom located at various surface sites on the GaAs (001)-$\beta 2(2\times 4)$ surface [see Fig. 1(a)].

Site	D_1	D_2	D_3	D_4	$D_{1\text{-BD}}$	$D_{2\text{-BD}}$	C_1	C_2	C_3	C_4	C_5	C_6
Energy	0.42	0.78	3.75	3.80	0.00	0.57	1.61	2.08	2.83	2.52	1.37	1.62

gated by estimating the adiabatic potential experienced by an isolated Au adatom interacting with the surface. A good approximation of this potential can be achieved by using the scheme outlined in previous theoretical studies.[14–18] An adatom is placed above the reconstructed surface in the x-y plane. It is kept fixed at a given (x,y) position, while all the substrate atoms and the z coordinate of the adatom are fully relaxed by following the atomic forces and by minimizing the total energy of the system. The relaxation procedure is repeated for all (x,y) positions of a regular grid, thus providing a mapping of the potential energy surface $E(x,y)$ (PES). In some (x,y) locations, the relaxation procedure has been repeated by starting with atomic geometries where the As-As dimer close to the Au atom is broken. This procedure should reveal the existence of deeper energy minima related to strong adatom-dimers interactions. Broken dimer (BD) configurations were found to play an important role in the case of Ga adatoms on the same GaAs(001)-$\beta 2(2\times 4)$ surface.[16,17] The Au binding sites and the energy barriers opposing the adatom diffusion have been identified by the local minima and the saddle points of the PES estimated for the Au adatom, respectively. The geometry and the total energy corresponding to the stable Au sites have been then refined by *fully relaxing* the geometry of the Au-surface system. In correspondence with the most interesting sites of the adatoms, the Au chemical binding has been investigated by analyzing the local geometry and the distribution of the (valence) electron charge density. In particular, two-dimensional (2D) contour plots of the electronic charge density have been analyzed together with 3D *difference density maps* that permit to reveal even small displacements of the electronic charge induced by bonding interactions between the interacting atoms.

Present results have revealed interesting characteristics of the Au-surface interaction that results to be quite different from the Ga-surface interaction. More specifically, in the case of the Ga adatom, the interaction of the Ga atom with the surface gives rise to two PES characterized by the presence and the absence of broken As-As dimers, respectively. On the other hand, only one PES may describe the interaction of an Au adatom with the GaAs surface, which is characterized by the absence of broken As-As dimers. This indicates that isolated Au adatoms *do not modify the surface reconstruction* in agreement with the results of a recent STM (scanning tunneling microscopy) investigation of depositions of fractions of a monolayer of gold on the reconstructed GaAs(001) surface[19] as well as with the absence of interdiffusion processes at low temperatures (i.e., below 400 °C).[7] The different behavior of the Ga and Au adatoms can be related to their different chemical bonding with the As atoms of the surface dimers. Ga atoms give rise to strong covalent Ga-As bonds characterized by a marked ionic character. The Au adatoms give rise instead to weaker *pure* covalent bonds. The nature of the Au binding favors the existence of different local minima on the PES and of different migration paths for the lateral diffusion of the Au atoms. An analysis of the energy barriers for the Au migration paths has shown two different activation energies for the Au diffusion along directions parallel or perpendicular to the As-As dimer rows. This indicates the existence of a *diffusional anisotropy* that should be observed by STM experiments and of interest for the technology of the Au-based contacts.

II. METHODS

In the Car-Parrinello method, the interatomic forces are computed from the instantaneous quantum-mechanical electronic ground state in the Born-Oppenheimer approximation. The electronic ground state corresponding to a given atomic geometry is obtained within the density-functional theory (DFT).[20,21] The exchange-correlation functional used in the calculations includes gradient corrections (GC) to the local-density approximation (LDA)[22,23] in the form proposed by Becke and Perdew.[24,25] Only the valence electrons are taken into account while the atomic inner cores are frozen. In the case of the Au atom, the interaction between the valence electrons and the frozen cores is described by soft first-principle pseudopotentials.[26] For Ga and As, we have used norm-conserving pseudopotentials.[27] The adatom-substrate system is modeled by supercell geometries with a (4×4) periodicity parallel to the surface. This periodicity has been tested to be sufficiently large to have negligible adatom-adatom interactions. Two different supercells have been used for the calculations that contain four and six layers of GaAs, respectively, plus an additional layer of H atoms that saturate the bonds of the lower surface. These supercells also contain a vacuum of six layers of GaAs perpendicular to the (001) surface. The four-layer supercell has been used for the calculation of the PES on a grid with a spacing of 1 Å as well as for refinements on a grid of 0.5 Å. The refinements were performed for the local minima and maxima identified by interpolating the former grid. In these calculations all the atoms of the substrate have been allowed to relax, but for the H atoms that are arranged in order to simulate a bulk-terminated configuration. Then, a geometry optimization with no constraints on the Au adatom has been performed for the most important local minima. The most interesting sites (e.g., the sites of Table I) and a small sample of other (x,y) locations chosen by taking into account the symmetry of the surface have been then investigated by using a larger supercell of six layers of GaAs plus an additional layer of H saturators. In these calculations, only the four layers of the substrate close to the surface were allowed to relax. The calculations performed with the larger supercells have concerned both a mapping on the finer grid around the above selected sites and geometry optimizations without any con-

straint on the minimum energy sites. The changes of the (relative) energy values on the PES due to the use of the six-layer supercells with respect to the four-layer supercells are within 0.1 eV. Further checks have been performed with a supercell of six layers of GaAs and a layer of pseudohydrogen saturators.[28] The achieved results are quite similar to those achieved by using the six-layer supercells with H saturators, although the use of pseudohydrogen saturators gives larger effects on the energy minima corresponding to the broken-dimer configurations. These energy minima have been lowered of about 0.2 eV. Further, the energy barrier evaluated for the broken-dimer configurations have been slightly increased by the presence of pseudo-H saturators. In summary, the use of six-layer supercells with pseudo-H saturators in place of four-layer supercells with H saturators induces a lowering of 0.2 eV of the energy minima corresponding to the BD sites and an almost rigid shift of the other local energy minima and maxima of the PES corresponding to the Au adatom. Even the local geometries (e.g., bond distances and bond angles) of the As-Au-As complexes are slightly affected by the use of different supercells and saturators. The results presented here, have been achieved by using four-layer supercells. Small corrections have been applied to the Au binding energies by taking into account the results achieved by using larger supercells. The single-particle Kohn-Sham wave functions have been expanded on a plane-wave basis set. As far as the kinetic-energy cutoff is concerned, the cutoffs of 16, 18, and 22 Ry have been tested. A satisfactory convergence of the results has been achieved by using a cutoff of 18 Ry. Only the Γ point is used for the **k**-space integration. The electronic optimization and structural relaxation have been performed using damped second-order dynamics with electronic-mass preconditioning scheme.[29]

Difference-density maps have been used here for an analysis of the chemical bonding of Au and Ga adatoms interacting with the surface As dimers. First, a charge-density sum $D_{\rm sum}$ is calculated, which is given by $D_{\rm surf}+D_{\rm atom}$. $D_{\rm surf}$ is the electronic density calculated for a supercell with no adatoms on the GaAs surface and where the As and Ga atoms are kept fixed at the positions they have in a given Au-surface configuration. $D_{\rm atom}$ is the electronic charge density relative to an isolated Au atom located at the coordinates corresponding to the same Au-surface configuration of $D_{\rm surf}$. Thus, $D_{\rm sum}$ represents the electronic density of the Au adatom and the surface when their interaction is ''switched off.'' Then, the charge density D for the Au-surface system is calculated. Difference densities D^- and D^+ are given by the negative and positive values of the difference $D-D_{\rm sum}$, respectively. When the Au-surface interaction is ''switched on'' and the electronic charge density is rearranged, the above difference has positive (negative) values where the electronic density increases (decreases), thus permitting a fine description of the Au-As interactions.

III. RESULTS AND DISCUSSION

A. Au chemical binding

The most interesting sites of an Au adatom on the GaAs (001)-$\beta 2(2\times 4)$ surface are shown in Fig. 1(a). Figure 1(b) shows a map of the PES calculated for the isolated Au adatom interacting with the surface together with the positions of some As-As dimers on the top and third layers. The PES topology is similar to that of the reconstructed GaAs surface. Regions characterized by two energy maxima separated by a deep energy minimum can be recognized around the As-As dimers of the top and third layers. These regions are separated by ''channels'' parallel and perpendicular to the direction of the dimer rows. In the above regions, the absolute energy minimum corresponds to a short-bridge site D_1 in Fig. 1(a), where the Au adatom forms an As-Au-As complex with a dimer of the third layer, see the atomic geometry shown in Fig. 2(a). A local minimum 0.36 eV higher in energy has been found at the D_2 site, which corresponds to a short-bridge site for a dimer of the top layer, see Figs. 1(a) and 3(a). The highest energy barriers correspond to the D_3 and D_4 sites, where the Au adatom is almost on the top of an As atom of a dimer. These sites are characterized by a strong repulsive interaction between the Au atoms and its nearest neighboring As atom. Further local minima and energy barriers are found in the channels around the dimers. For instance, the C_1 and C_2 sites are local minima and the C_3 and C_4 sites are saddle points. C_5 and C_6 sites are further local minima. The total energy values corresponding to the above sites are given in Table I. The Au adatom does not break the As-As dimers when located at the D_1 or D_2 binding sites. Broken dimer configurations have been investigated by estimating the binding energy of an Au adatom with its (x,y) coordinates fixed above a dimer center as a function of the height z_d with respect to the same center. In the case of dimers of the third layer, this procedure has found both the energy minimum corresponding to the D_1 site ($z_d=2.43$ Å) and a further energy minimum 0.42 eV lower in energy and closer to the dimer ($z_d=0.74$ Å). The latter energy minimum corresponds to a BD configuration, $D_{1\text{-BD}}$, see Fig. 4(a). The energy minima corresponding to the D_1 and $D_{1\text{-BD}}$ sites are separated by a barrier of 2.13 eV. Similarly, in the case of dimers of the top layer, a local energy minimum 0.21 eV lower in energy with respect to that of the D_2 site has been found for a BD configuration where z_d is equal to 1.50 Å, site $D_{2\text{-BD}}$, see Fig. 5(a). In this case, a barrier of 2.4 eV separates the two energy minima. Thus, the absolute energy minimum for the Au adatom corresponds to the $D_{1\text{-BD}}$ site, which has been assumed as the zero of energy in Table I.

The Au-dimer interaction has been compared with the interaction of Ga adatoms with the As dimers on the surface. Only the case of Ga atoms interacting with the dimers of the *top* layer will be discussed here, quite similar results have been achieved in the case of dimers of the third layer. Hereafter, X_2 and $X_{2\text{-BD}}$ represent the Ga binding sites corresponding to the D_2 and $D_{2\text{-BD}}$ Au sites, respectively. The atomic geometry relative to the $X_{2\text{-BD}}$ site is shown in Fig. 6(a). In agreement with previous theoretical results,[15,17] the $X_{2\text{-BD}}$ site corresponds to an energy minimum 1.1 eV lower in energy than that relative to the X_2 site. The two minima are separated by an energy barrier of 0.6 eV. These results indicate that the adatom-dimer interaction is quite different in the cases of the Ga and Au adatoms. In the case of Ga, the energy gain from the X_2 to the $X_{2\text{-BD}}$ configurations (1.1 eV)

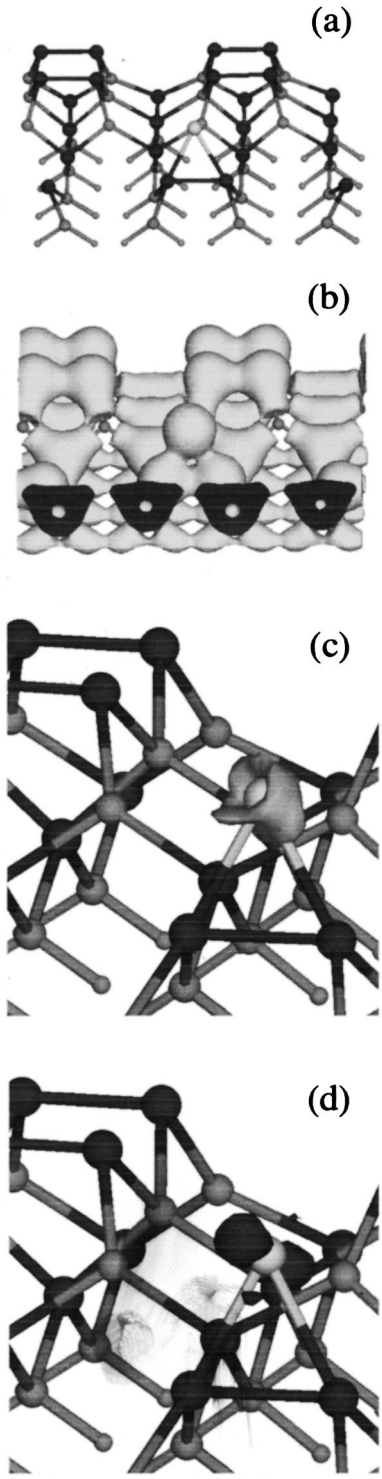

FIG. 2. The figure shows the geometry and some charge-density isosurfaces for an Au adatom located at the site D_1 of Fig. 1(a). (a) Atomic geometry, the As and Ga atoms are represented by black and gray spheres, respectively. The Au adatom is represented by the biggest gray sphere, the H atoms by the smallest spheres. (b) Total valence charge density, the isosurface corresponds to an electron density of 0.035 e/a.u.^{3}; (c) D^- density (see the text), the isosurface corresponds to an electron density of 0.010 e/a.u.^{3}; (d) D^+ density (see the text), the isosurface corresponds to an electron density of 0.010 e/a.u.^{3}

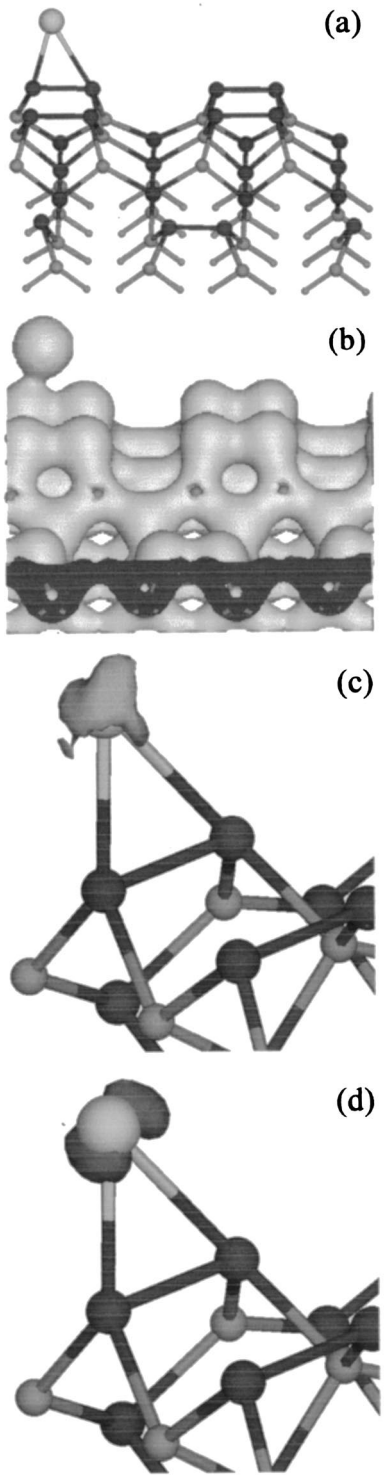

FIG. 3. The figure shows the geometry and some charge-density isosurfaces for an Au adatom located at the site D_2 in Fig. 1(a). (a) Atomic geometry, the As and Ga atoms are represented by black and gray spheres, respectively. The Au adatom is represented by the biggest gray sphere, the H atoms by the smallest spheres. (b) Total valence charge density, the isosurface corresponds to an electron density of 0.035 e/a.u.^{3}; (c) D^- density (see the text), the isosurface corresponds to an electron density of 0.010 e/a.u.^{3}; (d) D^+ density (see the text), the isosurface corresponds to an electron density of 0.010 e/a.u.^{3}

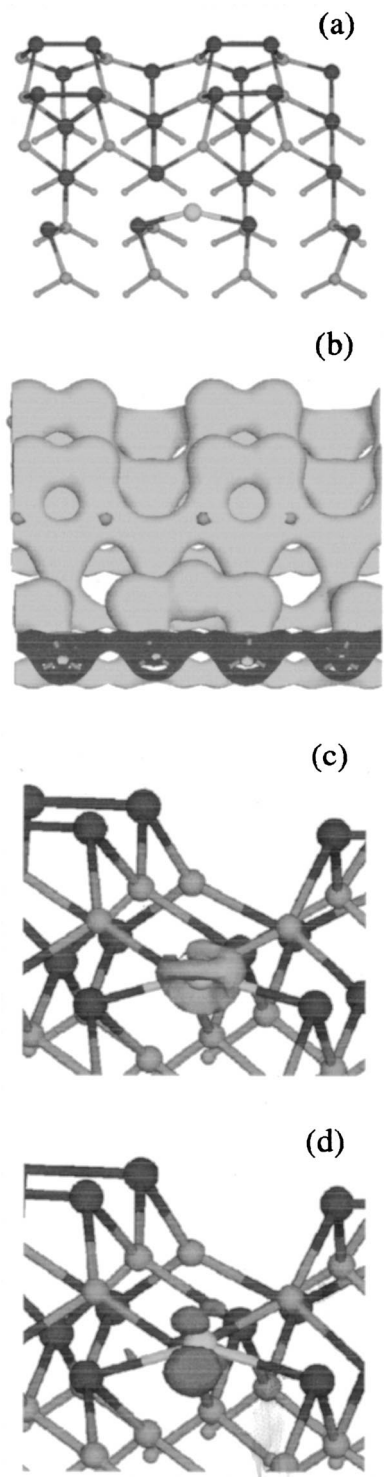

FIG. 4. The figure shows the geometry and some charge-density isosurfaces for an Au adatom located at the site $D_{1\text{-BD}}$ in Fig. 1(a). (a) Atomic geometry, the As and Ga atoms are represented by black and gray spheres, respectively. The Au adatom is represented by the biggest gray sphere, the H atoms by the smallest spheres. (b) Total valence charge density, the isosurface corresponds to an electron density of 0.035 e/a.u.^{3}; (c) D^- density (see the text), the isosurface corresponds to an electron density of 0.010 e/a.u.^{3}; (d) D^+ density (see the text), the isosurface corresponds to an electron density of 0.010 e/a.u.^{3}

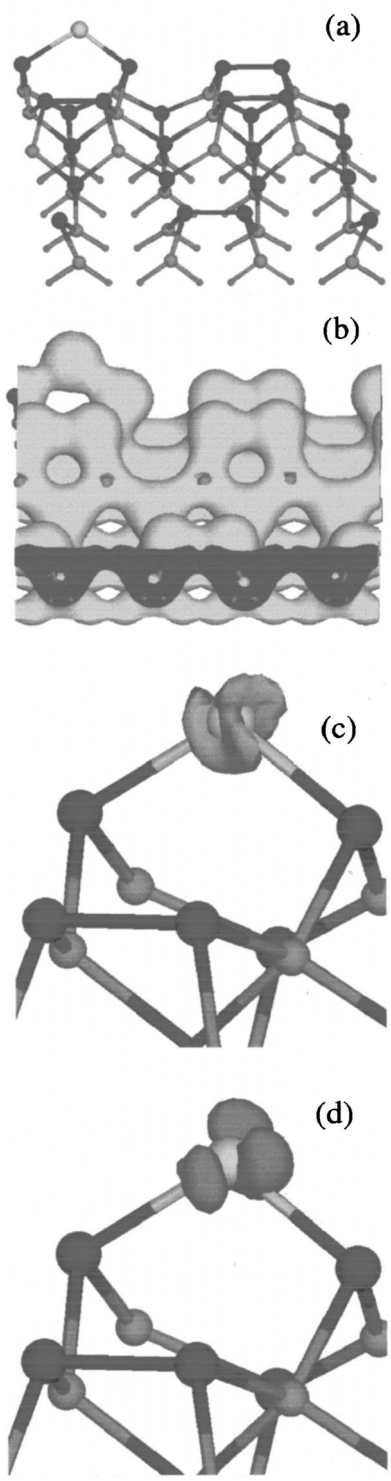

FIG. 5. The figure shows the geometry and some charge-density isosurfaces for an Au adatom located at the site $D_{2\text{-BD}}$ in Fig. 1(a). (a) Atomic geometry, the As and Ga atoms are represented by black and gray spheres, respectively. The Au adatom is represented by the biggest gray sphere, the H atoms by the smallest spheres. (b) Total valence charge density, the isosurface corresponds to an electron density of 0.035 e/a.u.^{3}; (c) D^- density (see the text), the isosurface corresponds to an electron density of 0.010 e/a.u.^{3}; (d) D^+ density (see the text), the isosurface corresponds to an electron density of 0.010 e/a.u.^{3}

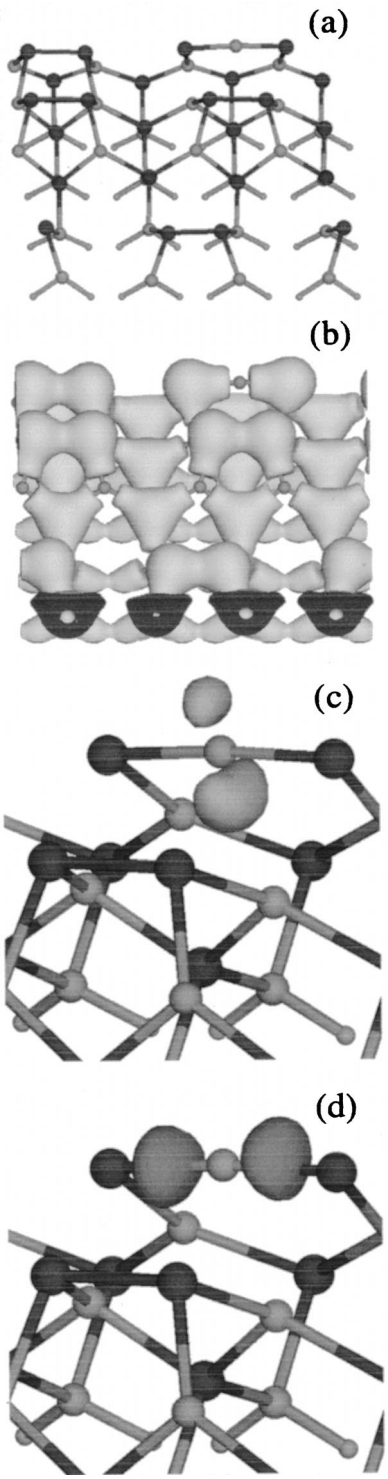

FIG. 6. The figure shows the geometry and some charge density isosurfaces for a Ga adatom located at the site $X_{2\text{-BD}}$ [corresponding to the site $D_{2\text{-BD}}$ in Fig. 1(a)]. (a) Atomic geometry, the As and Ga atoms are represented by black and gray spheres, respectively. The H atoms are represented by the smallest spheres. (b) Total valence charge density, the isosurface corresponds to an electron density of 0.035 e/a.u.^{3}; (c) D^- density (see the text), the isosurface corresponds to an electron density of 0.010 e/a.u.^{3}; (d) D^+ density (see the text), the isosurface corresponds to an electron density of 0.010 e/a.u.^{3}

TABLE II. Atomic distances (angstroms) in the geometries of the As-Au-As and As-Ga-As complexes formed by Au and Ga adatoms located at short-bridge sites of an As-As dimer, see Figs. 1–6. M represents an Au adatom located at the D sites or a Ga adatom located at the X sites. BD stands for broken-dimer configurations (see the text). As_1 and As_2 represent the atoms of an As dimer. z_d indicates the distance of the Au or Ga adatoms from the center of the As dimer.

Site	M-As_1	M-As_2	As_1-As_2	z_d
D_1	2.79	2.77	2.67	2.43
D_2	3.00	3.41	2.53	2.91
$D_{1\text{-BD}}$	2.58	2.53	4.98	0.74
$D_{2\text{-BD}}$	2.88	2.70	4.66	1.50
$X_{2\text{-BD}}$	2.26	2.27	4.52	0.14
X_2	2.72	2.72	2.52	2.40

is much larger than those corresponding to the D_2 and $D_{2\text{-BD}}$ configurations (0.21 eV) and to the D_1 and $D_{1\text{-BD}}$ configurations (0.42 eV). Further, in the case of Au adatoms, much higher energy barriers separate the minima corresponding to the non-BD and BD configurations with respect to the case of Ga adatoms. Thus, at variance with the case of Ga adatoms, only the PES corresponding to unbroken As-As dimers can be used to describe the interaction of Au adatoms with the GaAs surface. That PES is shown in Fig. 1(b).

The comparison between the Au-dimer interaction and the Ga-dimer interaction has been extended to the characteristics of the chemical bonding of the two adatoms in the BD configurations. In detail, the chemical bonding has been carefully investigated by analyzing the geometries and the total and difference charge-density maps of the As-Au-As and As-Ga-As complexes corresponding to the $X_{2\text{-BD}}$, $D_{2\text{-BD}}$, and $D_{1\text{-BD}}$ configurations. For sake of clearness, the results achieved for the As-Ga-As complex will be discussed first. In the As-Ga-As complexes, the Ga-As distances are smaller in the BD configuration, where the complex has an almost ''on-line'' geometry, with respect to the non-BD one, see Table II. Moreover, the Ga-As distances reach values (2.27 Å) smaller than that estimated by the atomic covalent radii,[30] 2.46 Å, thus indicating the existence of a strong Ga-As bonding interaction. First, the nature of the chemical bonds formed in the As-Ga-As complexes has been investigated by analyzing the total (valence) electronic charge-density distributions. In this analysis, the distribution of the electronic charge around the As atoms of an isolated dimer has been taken as indicative of the formation of covalent bonds. The As-As dimers on the surface are characterized indeed by As-As distances of 2.51 Å, to be compared with the value of 2.4 Å estimated by the As covalent radius.[30] The largest charge-density value that permits to appreciate the formation of the As-As covalent bonds in the isolated dimers has been used, therefore, to calculate all the total charge-density isosurfaces discussed in the present study. An isosurface of the total charge density corresponding to the As-Ga-As geometry of Fig. 6(a) is shown in Fig. 6(b). This isosurface shows a piling up of the electronic charge density on the As atoms neighboring the Ga atom that implies the formation of cova-

lent bonds with a marked ionic character. This electronic distribution should be compared with that found for an Au adatom located at the $D_{2\text{-BD}}$ site, see Fig. 5(b), which suggests the formation of pure covalent Au-As bonds. The different nature of the chemical bonds in the two above As-Ga-As and As-Au-As configurations is confirmed by 2D contour plots of the (valence) electronic density and 3D isosurfaces of the difference maps. Figures 7(a) and 7(b) show contour plots of the electronic density in planes orthogonal to the surface and close to the atoms of the As-Ga-As ($X_{2\text{-BD}}$ configuration) and As-Au-As ($D_{2\text{-BD}}$ configuration) complexes, respectively. Figure 7(a) confirms the ionic character of the Ga-As bonds. Figure 7(b) suggests the formation of an Au-As covalent bond. The same figure shows that only one contour line surrounds the Au and As atoms, while two lines surround the As-As atoms of a neighboring dimer located on the same plane of the contour plot [see also the As-Au-As geometry in Fig. 5(a)]. This suggests the formation of Au-As covalent bonds weaker than the Ga-As bonds. Even the difference density maps relative to the Ga adatom, see Figs. 6(c) and 6(d), show a marked displacement of the electronic charge from the Ga atom towards its As neighbors, when the adatom-dimer interaction is ''switched on.'' A quite different electronic distribution characterizes the chemical bonding of the Au adatoms. The difference density maps of Figs. 5(c) and 5(d) show indeed the absence of charge displacements from the Au atom toward its As neighbors. The nature of the Au chemical bonding can be clarified by an analysis of all the above charge-density plots. Figures 5(b) and 7(b) show the presence of some electronic charge between the Au and As atoms, thus indicating a covalent nature of the Au-As bonds. Figures 5(c) and 5(d) indicate that the formation of those covalent bonds does not imply a displacement of charge from the Au adatom toward its As neighbors, thus indicating the formation of pure covalent bonds. The above analysis of the Au chemical bonding at the $D_{2\text{-BD}}$ site may be related to the geometry of the As-Au-As complex, see Table II. At variance with the case of Ga, the Au-As distances are both larger than the value estimated from the covalent radii 2.6 Å, thus suggesting the formation of weak Au-As bonds. Finally, a different strength of the As-Ga-As and As-Au-As bonds is suggested by an estimate of the dissociation energy $\Delta E = E(\text{adatom}+\text{surface}) - E(\text{surface}) - E(\text{atom})$. Values of ΔE equal to 2.7 and 1.13 eV have been indeed calculated for the $X_{2\text{-BD}}$ and $D_{2\text{-BD}}$ configurations, respectively. Although the above procedure gives only a rough estimate of the dissociation energies, the above ΔE values favorably compare with the energy required to break an isolated As dimer (on the top layer), which has been estimated to be equal to 1.3 eV. In the case of the other investigated Au broken-dimer configuration, $D_{1\text{-BD}}$, present results indicate the formation of Au-As covalent bonds stronger than those formed in the $D_{2\text{-BD}}$ configuration. The corresponding dissociation energy is equal to 1.7 eV. The geometry of this configuration shows a symmetrical location of the Au adatom with respect to the As atoms of the broken dimer. Moreover, the Au-As distances are close to the value estimated from the covalent radii, see Table II. The charge-density distributions shown in the Figs. 4(b) and 7(d) indicate an increase of the electronic

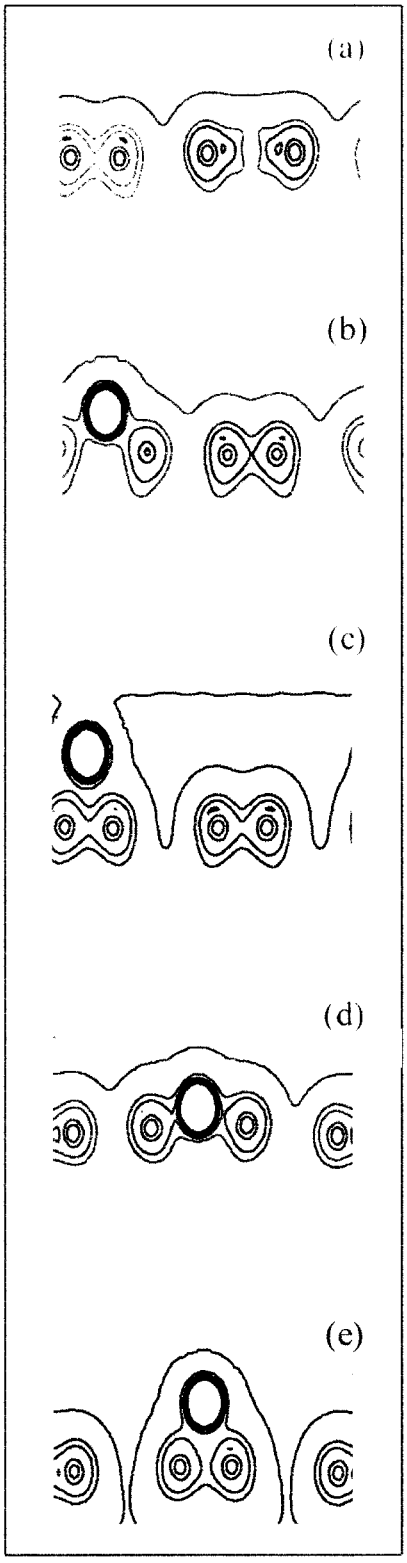

FIG. 7. Contour plots in planes perpendicular to the GaAs surface and close to the atoms of the As-Ga-As complex [Fig. 7(a)] or As-Au-As complexes [Figs. 7(b–e)]. Contour lines correspond to seven equidistant levels in the range 0.0–0.186 e/a.u.^{3} (a) $X_{2\text{-BD}}$ site; (b) $D_{2\text{-BD}}$ site; (c) D_2 site; (d) $D_{1\text{-BD}}$ site; (e) D_1 site. See Figs. 2–6 for the different geometries of the As-Ga-As and As-Au-As complexes.

charge between the Au and As atoms with respect to the $D_{2\text{-BD}}$ configuration. However, once more, the difference maps of Figs. 4(c) and 4(d) show the absence of a charge displacement from the Au atom towards its As neighbors, thus confirming the covalent character of the As-Au-As bonds.

For what concerns the non-BD configurations, the geometries of the corresponding As-Au-As complexes are also given in Table II. In the case of the D_1 site, the Au adatom is located midway between the As atoms, it is closer to one of the As atoms of the dimer in the case of the D_2 site. The shortest Au-As distances are equal to 2.77 and 3.00 Å in the D_1 and D_2 configurations, respectively, to be compared with the value estimated by the covalent radii, 2.6 Å. The Au-As distances are shorter and the As-As distances are longer in the case of the D_1 site with respect to the D_2 site. Similar results have been found in the cases of the $D_{1\text{-BD}}$ and $D_{2\text{-BD}}$ sites. This suggests that the As dimers of the third layer are more reactive than those of the top layer, in agreement with the existence of the lower-energy minima in correspondence of the D_1 and $D_{1\text{-BD}}$ sites. This result can be accounted for by the different binding of the Ga atoms neighboring the dimers. In the case of the D_2 site, the Ga atoms carry a dangling bond and are threefold coordinated. They may relax, therefore, by following the displacements of the As atoms forming the dimers. In fact, the corresponding Ga-Ga distances reach the value of 3.6 Å against the value of 4.0 Å found in the bulk, thus stabilizing the As dimer. On the other hand, in the case of the D_1 site, the Ga atoms neighboring the dimers are fourfold coordinated and the corresponding Ga-Ga distance is about 4.0 Å. These Ga atoms do not follow the displacements of the As atoms forming the dimers that result to be the more reactive ones. The longer Au-As distances characterizing the non-BD configurations with respect to the BD ones indicate the formation of weaker Au-As bonds. This agrees with the smaller dissociation energies—1.28 and 0.92 eV for the D_1 and D_2 configurations, respectively—estimated for the non-BD configurations with respect to the BD configurations. The formation of weaker Au-As bonds in the D_1 and D_2 configurations is confirmed by an analysis of the corresponding charge-density distributions. In the case of the D_1 configurations, Figs. 2(b) and 7(e) should be compared with Figs. 4(b) and 7(d) (which correspond to the $D_{1\text{-BD}}$ configuration), respectively. These figures show a decrease of charge density between the Au and As atoms on going from the $D_{1\text{-BD}}$ to the D_1 configurations. For the same two configurations, the difference maps—Figs. 4(c) and 4(d) for the $D_{1\text{-BD}}$ site, Figs. 2(c) and 2(d) for the D_1 site—confirm the absence of a charge displacement from the Au atom to its As neighbors. It should be noted that the small differences between the charge distribution of the D_1 and $D_{1\text{-BD}}$ configurations, Figs. 7(d) and 7(e), respectively, agree with the small difference between the corresponding total energies (0.42 eV). A quite similar analysis can be performed in the cases of the D_2 and $D_{2\text{-BD}}$ configurations.

All the above results can be included in a coherent picture. An Au adatom has the strongest bonding interactions with the surface atoms when it is located at short-bridge sites of the As dimers. A similar result has been found in the case of the Ga adatoms. However, the nature of the Au chemical binding is quite different from that of the Ga adatom. The adatom-dimer interaction is characterized indeed by the formation of covalent Ga-As bonds with a marked ionic character in the case of Ga and by the formation of weaker covalent Au-As bonds in the case of Au adatoms. The different chemical binding of the two adatoms accounts for the higher barriers that the Au adatom must overcome to break an As dimer with respect to the Ga adatom. In fact, the energy required to break an isolated As dimer on the top layer is equal to 1.3 eV. The barriers found for the formation of the BD configurations are higher and lower than 1.3 eV in the case of Au and Ga adatoms, respectively, because the latter atom has stronger bonding interactions with the As dimers. In particular, the energy barriers estimated for the formation of BD configurations in the case of Au adatoms are about three times larger than those found in the case of the Ga adatoms. In the case of gold, the formation of BD configurations will require, therefore, high-temperature conditions in order to favor the breaking of the As dimers. This suggests that the presence of Au adatoms does not modify the $\beta 2(2\times 4)$ reconstruction pattern of the GaAs surface and agrees with the results of a recent STM investigation of depositions of fractions of a monolayer of gold on the reconstructed GaAs(001) surface.[19] The above results also agree with the absence of interdiffusion processes at low temperatures.[7] Finally, the lower reactivity of the Au adatom with respect to that of Ga agrees with the different effects that the BD configurations have on the corresponding PES, negligible in the case of Au adatoms, significant in the case of Ga adatoms.

B. Migration paths

On the ground of the above results, only the PES calculated for the non-BD configurations has been considered in the analysis of the Au migration paths on the GaAs surface. These migration paths have been investigated within the framework of the transition-state theory.[31] This approach requires to determine the activation energy for a jump between two binding sites. A number of possible paths has been considered by taking into account the topology of the PES of Fig. 1(b), which induces to examine diffusion paths in directions parallel and perpendicular to the dimer rows. The activation energy for Au diffusion along these paths has been estimated by examining the local minima and the saddle points of the PES. This analysis has shown that the activation energies for the Au migration range from 0.6 to 3.6 eV and from 1.1 to 2.2 eV in directions parallel and perpendicular to the dimer rows, respectively. These results, in particular, the existence of an energy barrier of only 0.6 eV, support the existence of a strong anisotropy in the two directions. This anisotropy is directly related to the characteristics of the Au-dimer bonding interaction and to the positions of the As dimers on the reconstructed surface. As an example, a migration path along the line of the C_3, C_2, C_4, C_2, and C_3 sites of Fig. 1(a) is characterized by energy barriers lower than 0.6 eV. On the other hand, along a path involving the C_1, C_4, C_1, C_5 and C_6 sites (which is almost perpendicular to the

dimer rows), the energy barriers are higher than 1.1 eV. Even a qualitative analysis of the PES of Fig. 1(b) immediately shows the existence of ''channels'' of an almost homogeneous color only in a direction parallel to the dimer rows. In a theoretical study of Si adatoms on the Si (100) surface, activation energies of 0.6 and 1.0 eV have been estimated for Si diffusion along and perpendicular to the dimer rows, respectively.[14,15] From these results, root-mean-square displacements of 10^3 Å and 1 Å, respectively, have been estimated for the Si adatoms at room temperature for a time of 10^2 s, which is a reasonable time between two observations in an STM experiment. Those theoretical predictions have been confirmed by STM experiments.[15,32] Present results suggest, therefore, that also in the case of the Au adatoms a dominant motion of the Au atoms parallel to the dimer rows should be revealed by STM experiments.

IV. CONCLUSIONS

In this work we have clarified the nature of the Au chemical binding for an isolated Au adatom on the GaAs (001)-$\beta 2(2\times4)$ reconstructed surface. The most interesting Au binding sites are located at short-bridge sites close to the As-As dimers of the top and third layers. Similar binding sites have been found for Ga adatoms. However, a Ga adatom forms covalent Ga-As bonds with a marked ionic character when interacting with the As dimers. The Au-dimer interaction is characterized instead by the formation of weaker (pure) covalent Au-As bonds. Accordingly, Au adatoms do not induce a breaking of the As-As dimers and do not affect the surface reconstruction. The migration of the Au adatoms on the surface should be faster in directions parallel to the dimer rows than perpendicular to them. This strong anisotropy of the Au diffusion should be observed by STM experiments and of interest for technological applications.

ACKNOWLEDGMENT

It is a pleasure to acknowledge G. Scavia for very helpful discussions.

*To whom the correspondence should be addressed
[1] T. C. Shen, G. B. Gao, and H. Morkoc, J. Vac. Sci. Technol. B **10**, 2113 (1992).
[2] K. Bock and H. L. Hartnagel, Semicond. Sci. Technol. **9**, 1005 (1994).
[3] M. Y. Lee and P. A. Bennett, Phys. Rev. Lett. **75**, 4460 (1995).
[4] J. D. O'Mahony, F. M. Leibsle, P. Weightman, and C. F. J. Flipse, Surf. Sci. **277**, L58 (1992).
[5] J. M. Carpinelli and H. H. Weitering, Phys. Rev. B **53**, 12 651 (1996).
[6] Z. Ma and L. H. Allen, Phys. Rev. B **48**, 15 484 (1993).
[7] D. Y. Noh, Y. Hwu, H. K. Kim, and M. Hong, Phys. Rev. B **51,** 4441 (1995).
[8] J. E. Northrup and Sverre Froyen, Phys. Rev. Lett. **71**, 2276 (1993).
[9] J. E. Northrup and Sverre Froyen, Phys. Rev. B **50**, 2015 (1994).
[10] L. Daweritz and R. Hey, Surf. Sci. **236**, 15 (1990).
[11] T. Hashizume *et al.*, Phys. Rev. Lett. **73**, 2208 (1994).
[12] R. Car and M. Parrinello, Phys. Rev. Lett. **55**, 2471 (1985).
[13] For a recent review see, D. Marx and J. Hutter, in *Modern Methods and Algorithms of Quantum Chemistry*, edited by J. Grotendorst (John Von Neumann Institute for Computing, Jülich, 2000), Vol. 1.
[14] G. Brocks, P. J. Kelly, and R. Car, Phys. Rev. Lett. **66**, 1729 (1991).
[15] G. Brocks, P. J. Kelly, and R. Car, Surf. Sci. **269/270**, 860 (1992).
[16] A. Kley and M. Scheffler, in *Proceedings of the 23rd International Conference on the Physics of Semiconductors*, edited by M. Scheffler and R. Zimmerman (World Scientific, Singapore, 1996), p. 1031.
[17] A. Kley, P. Ruggerone, and M. Scheffler, Phys. Rev. Lett. **79**, 5278 (1997).
[18] M. A. Salmi, M. Alatalo, T. Ala-Nissila, and R. M. Nieminen, Surf. Sci. **425**, 31 (1999).
[19] A. Amore Bonapasta, G. Scavia, and F. Buda (unpublished).
[20] R. G. Parr, W. Yang, *Density Functional Theory of Atoms and Molecules* (Oxford Univesity Press, New York, 1989).
[21] R. O. Jones and O. Gunnarson, Rev. Mod. Phys. **61**, 689 (1989).
[22] J. P. Perdew and A. Zunger, Phys. Rev. B **23**, 5048 (1981).
[23] D. M. Ceperley and B. J. Alder, Phys. Rev. Lett. **45**, 566 (1980).
[24] A. D. Becke, Phys. Rev. A **38**, 3098 (1988).
[25] J. P. Perdew, Phys. Rev. B **33**, 8822 (1986).
[26] D. Vanderbilt, Phys. Rev. B **41**, 7892 (1990).
[27] R. Stumpf, X. Gonze, and M. Scheffler, Fritz-Haber-Institut Research Report No. 1, 1990 (unpublished).
[28] K. Shiraishi, J. Phys. Soc. Jpn. **59**, 3455 (1990).
[29] F. Tassone, F. Mauri, and R. Car, Phys. Rev. B **50**, 10 561 (1994).
[30] The values of the covalent radii, in angstroms, are 1.26 (Ga), 1.20 (As), and 1.40 (Au), see J. C. Phillips, *Bonds and Bands in Semiconductors* (Academic, New York, 1973), p. 21.
[31] G. H. Vineyard, J. Phys. Chem. Solids **3**, 121 (1957).
[32] Y. W. Mo and M. G. Lagally, Surf. Sci. **248**, 313 (1991).